

# Geometry-Based Intravitreal Pharmacokinetics: A Theoretical Pharmacokinetic Modeling Study Using Triamcinolone Acetonide and Vancomycin as Representative Intravitreal Agents

Andreas F Borkenstein <sup>1</sup>, Eva-Maria Borkenstein<sup>1</sup>, Rodrigo Pessoa Cavalcanti Lira<sup>2</sup>

<sup>1</sup>Borkenstein & Borkenstein Research & Laboratory Gmbh, Privatklinik der Kreuzschwestern, Graz, Austria; <sup>2</sup>Universidade Federal de Pernambuco, Recife, Pernambuco, Brazil

Correspondence: Andreas F Borkenstein, Borkenstein & Borkenstein Research & Laboratory GmbH, Privatklinik der Kreuzschwestern, Graz, Austria, Email [crustalith@gmx.at](mailto:crustalith@gmx.at)

**Purpose:** To quantify how anatomical variation in vitreous cavity volume, estimated from axial length (AL) using the VIVEX formula, influences intravitreal drug concentration, therapeutic exposure duration, and immediate intraocular pressure (IOP) dynamics under fixed-dose intravitreal therapy.

**Patients and Methods:** This theoretical pharmacokinetic modeling study utilized the VIVEX equation  $\{V = (\pi/6) \times AL^3 \times [0.76 + 0.012(AL - 24)]\}$  to calculate vitreous volume (VV) for three representative eye types: small hyperopic (AL 20 mm), emmetropic (AL 23.5 mm), and large myopic (AL 30 mm). A one-compartment first-order elimination model was applied to two commonly used intravitreal agents: triamcinolone acetonide (4 mg) and vancomycin (1 mg). Primary outcomes included initial concentration ( $C_0$ ), duration above therapeutic threshold ( $t_{eff}$ ), and modeled acute IOP rise. A Monte-Carlo simulation (10,000 virtual eyes) was performed to estimate population-level variability.

**Results:** Modeled VV increased from 2.98 mL (AL 20 mm) to 11.76 mL (AL 30 mm), producing an approximately fourfold difference in  $C_0$ . For triamcinolone,  $C_0$  decreased from 1.34 to 0.34 mg/mL and  $t_{eff}$  decreased from 67.4 to 31.8 days ( $\approx 50\%$  reduction). For vancomycin,  $C_0$  decreased from 0.336 to 0.085 mg/mL and  $t_{eff}$  decreased from 9.1 to 6.1 days. Predicted immediate IOP elevations were  $\sim 4.3$  mmHg in small eyes versus  $\sim 1.1$  mmHg in large eyes. Monte Carlo analysis suggested that anatomical variability accounts for  $\sim 30\%$  of modeled pharmacokinetic variance.

**Conclusion:** Anatomical differences in VV substantially and predictably influence intravitreal pharmacokinetics. The modeled results demonstrate that fixed intravitreal dosing leads to substantial geometry-driven differences in drug exposure across eye sizes. Fixed dosing strategies may increase peak exposure and IOP load in small eyes and shorten effective therapeutic duration in large myopic eyes. Biometry-stratified clinical studies are warranted to validate these modeling predictions and to assess their clinical relevance in intravitreal antibiotic and corticosteroid therapies.

**Keywords:** intravitreal pharmacokinetics, individual vitreous volume, axial length, individualized dosing, triamcinolone and vancomycin, vivex formula

## Introduction

Intravitreal injection therapy has become one of the most frequently performed procedures in modern ophthalmology.<sup>1,2</sup> Over the past two decades, it has profoundly changed the management of retinal diseases by enabling effective, localized treatment of conditions that previously led to irreversible vision loss. Intravitreal injection therapy has become a cornerstone of modern retinal disease management, with anti-VEGF agents, corticosteroids and antibiotics widely used across multiple indications.<sup>3-6</sup>

However, despite all these advances, intravitreal therapy remains largely standardized in 2025: all patients, regardless of ocular size or anatomical configuration, receive the same injection volume and dose of a medication; this is currently irrespective of individual ocular geometry.<sup>7–9</sup>

However, the vitreous cavity, which constitutes approximately 80% of the total eye globe, shows considerable interindividual variability. Numerous studies showed that this variation is primarily determined by the axial length (AL) of the eye, an easily measurable biometric parameter that strongly correlates with vitreous cavity volume.<sup>10,11</sup> One study measured the vitreous chamber volume (VCV) using computed tomography (CT) and stated that the VCV appeared to be greater than the current consensus suggests. The authors also suggested that the VCV is associated with age and axial length, indicating that it is dynamic and may change throughout adulthood and that the information regarding the volume of the vitreous chamber is useful for the understanding of proper dosage and behavior of agents that are inserted into the vitreous chamber.<sup>12</sup>

A small hyperopic eye (AL  $\approx$  20 mm, refraction  $\approx$  +5 D) typically contains around 3 mL of vitreous fluid, whereas an emmetropic eye (AL  $\approx$  23.5 mm) holds  $\approx$ 4–5 mL, and a highly myopic eye (AL  $\approx$  30 mm, refraction  $\approx$  –9 D) can reach >11 mL.<sup>13–15</sup> In a recent study estimating individual vitreous volumes using axial-length–based modeling, eyes with the largest estimated volumes showed significantly lower immediate IOP rises after anti-VEGF injection compared to eyes with smaller volumes.<sup>16</sup> Recently a study showed that tailoring intravitreal drug and gas dosages according to axial length and vitreous cavity volume might enhance intraocular drug distribution, potentially improving both safety and therapeutic outcomes. Authors of this study recommended dose adjustments for small eyes, administering 70–80% of the standard dose; for large eyes, 130–140%; and for extra-large eyes, 170–180% of the standard dose.<sup>17</sup> Another study evaluated the intravitreal concentration of vascular endothelial growth factor (VEGF) in dependence of the axial length in eyes without intraocular neovascularization and concluded that intravitreal VEGF concentration decreases with increasing axial length. They confirmed a kind of diluting effect in eyes with larger intraocular volume and/or a faster turnover rate of VEGF in axially myopic eyes with vitreous liquefaction.<sup>18</sup> The recently developed VIVEX formula provides a simple but anatomically accurate way to estimate the vitreous volume of an individual eye using its axial length:  $V = (\pi/6) \cdot AL^3 \cdot [0.76 + 0.012(AL - 24)]$ . This equation corrects the idealized spherical volume so that it fits better to the real anatomical proportions of the eye, and it has also been validated with MRI-based volume measurements, which showed very good agreement.<sup>13,15</sup> By translating a basic biometric parameter into a physiological volume, the VIVEX formula may offer a bridge between geometric anatomy and intravitreal pharmacology.

From a geometric perspective, ocular volume scales approximately with the cube of axial length. However, the pharmacokinetic implications of this volumetric scaling have not previously been systematically quantified. Pharmacokinetic behavior within the eye is complicated and depends not only on drug-specific properties, such as molecular weight, lipophilicity, and binding affinity, but also on the volume of distribution and clearance pathways within the vitreous body.<sup>19–21</sup>

Intravitreal dosing regimens, including those established in pivotal clinical trials and regulatory approvals, apply standardized injection volumes irrespective of ocular size. In this theoretical study, we apply the VIVEX model to simulate drug pharmacokinetics in eyes of different sizes and refractive categories. To illustrate geometry-dependent pharmacokinetic scaling across distinct molecular classes, we selected two clinically established intravitreal agents with fundamentally different properties: triamcinolone acetonide, a lipophilic corticosteroid with depot-like behavior, and vancomycin, a hydrophilic antibiotic with short intravitreal half-life. These agents represent contrasting clearance mechanisms and exposure dynamics, enabling a structured evaluation of volume-dependent effects.

These substances encompass a broader range of molecular weights, half-lives, and diffusion properties, enabling an evaluation of both short- and long-acting agents. By integrating the VIVEX-derived vitreous volumes into a pharmacokinetic model and validating it through Monte Carlo simulation, regression analysis, and comparison with published data, this work aims to quantify the impact of ocular size on drug concentration, exposure, and IOP dynamics.

Ultimately, the goal of this research is to establish a mathematical and translational foundation for individualized dosing in intravitreal therapy and future clinical studies. This work is intended to serve as a kind of starting point for the design of better-structured clinical trials that explicitly account for anatomical variability. The aim of the study is that future research based on this concept could help to systematically evaluate how vitreous volume influences both

therapeutic efficacy and potential adverse events, such as transient IOP spikes, localized toxicity from overexposure in small hyperopic eyes, or subtherapeutic dosing and shortened retreatment intervals in large myopic eyes.

## Methods

### Anatomical Modeling

The anatomical basis of this theoretical modeling simulation was the estimation of the vitreous cavity volume (VV) for eyes of different sizes using the VIVEX formula, a geometry-based model that relates axial length (AL) to total vitreous volume while correcting for natural deviations from the spherical shape of the human eye. The formula is defined as:  $V = AL^3 \cdot (\pi/6) \cdot [0.76 + 0.012(AL - 24)]$  where V is expressed in cubic millimeters and converted to milliliters by dividing by 1000, and AL represents the axial length in millimeters. The coefficient 0.76 and correction term  $0.012 \times (AL - 24)$  are derived from empirical fits to human MRI and optical biometry data, providing an accurate approximation of real-world vitreous dimensions across a broad biometric spectrum.<sup>13</sup> This geometric model compensates for the known aspheric elongation of the globe in myopia and the compression in hyperopia.<sup>22</sup> For example, a 1 mm change in axial length corresponds approximately to a 0.35 mL change in vitreous volume in the physiological range between 20 mm and 30 mm AL.

The VIVEX formula does not explicitly adjust for lens status (phakic versus pseudophakic). However, the influence of cataract extraction on vitreous cavity volume seems negligible, as the thicker crystalline lens is replaced by an intraocular lens of slightly thinner volume. Postoperatively, the principal anatomical change occurs more in anterior chamber depth rather than in vitreous cavity dimensions; this aspect has been discussed previously in the context of VIVEX.<sup>15</sup>

To capture the full range of anatomical variation observed in clinical practice, three representative eye types were modeled as the structural basis for all subsequent pharmacokinetic simulations. These categories correspond to the most clinically relevant extremes of axial length and refractive state found in the general population:

- Small hyperopic eye (AL = 20 mm; refractive error  $\approx +5$  D): VV = 2.98 mL
- Normal emmetropic eye (AL = 23.5 mm): VV = 5.12 mL
- Large myopic eye (AL = 30 mm; refractive error  $\approx -9$  D): VV = 11.76 mL

We believe the use of the selected three model eyes as realistic geometric archetypes representing the hyperopic, emmetropic, and myopic extremes of the population. This stepwise approach also mirrors the distribution of axial lengths observed in large epidemiologic cohorts such as the Beijing Eye Study and the UK Biobank, where approximately 70% of adults are emmetropic (AL  $\approx 23$ –25 mm), 15–20% are mildly hyperopic and 10–15% exhibit myopia or high myopia.<sup>23</sup>

For all subsequent pharmacokinetic simulations, these three vitreous volumes were used as fixed anatomical constants representing the functional distribution of eye sizes encountered in real-world intravitreal therapy.

Modeling these categories allows the analysis to span the practical limits of ocular geometry, ensuring that pharmacokinetic predictions reflect the variability clinicians face when treating patients with hyperopia, emmetropia, or high myopia.

### Pharmacokinetic Framework

Drug concentration over time was modeled using a first-order exponential elimination function:  $C(t) = (D/V) \cdot e^{(-kt)}$ , where  $C(t)$  denotes the drug concentration (mg/mL) at time  $t$  (days),  $D$  is the injected dose (mg),  $V$  is the vitreous volume (mL) derived from the VIVEX formula, and  $k$  is the elimination rate constant defined by  $k = \ln(2) / t_{1/2}$ . The model assumes first-order elimination kinetics, which have been validated for most intravitreal compounds in both experimental and clinical pharmacokinetic studies.<sup>24–27</sup> The initial concentration ( $C_0$ ) was defined as  $C_0 = D/V$ . The elimination rate constant was calculated as  $k = \ln(2)/t_{1/2}$ , where  $t_{1/2}$  represents the intravitreal half-life of the respective drug. The effective duration of action ( $t_{\text{eff}}$ ) was defined as the time during which the modeled concentration remained above a predefined

pharmacodynamic threshold ( $C_{\text{thresh}}$ ). Under first-order elimination, this was calculated analytically as:  $t_{\text{eff}} = \ln(C_0 / C_{\text{thresh}}) / k$ . For triamcinolone acetonide, the pharmacodynamic threshold concentration ( $C_{\text{thresh}}$ ) was set to 0.1 mg/mL. For vancomycin,  $C_{\text{thresh}}$  was defined as the minimum inhibitory concentration (MIC) of 0.005 mg/mL (5  $\mu\text{g/mL}$ ), representing a clinically relevant target for gram-positive coverage.

A simulation period of 0–60 days was chosen to encompass both short-acting (antibiotic) and long-acting (corticosteroid) pharmacokinetic profiles. For the model we assumed that the drug is fully dissolved and also evenly distributed in the vitreous cavity after the injection, because this is shown like that in several imaging and pharmacodynamics studies, which demonstrate rapid equilibration within minutes in nonvitrectomized eyes.<sup>28</sup> The Vitreous Therapeutic Index (TI) was defined as the ratio between initial concentration and pharmacodynamic threshold:  $\text{TI} = C_0 / C_{\text{thresh}}$ . The area under the concentration–time curve (AUC) was derived analytically from the first-order elimination equation.

## Monte Carlo Simulation

To estimate the impact of biometric variability at the population level, a Monte Carlo simulation was performed using 10,000 iterations. Axial length (AL) values were randomly sampled from a normal distribution with mean 23.5 mm and standard deviation 2.5 mm, reflecting population-based biometric data. For each simulated eye, vitreous volume was calculated using the VIVEX equation. Drug concentration–time profiles were generated analytically using the first-order elimination model. Output variables included initial concentration ( $C_0$ ), area under the concentration–time curve (AUC), and effective duration above threshold ( $t_{\text{eff}}$ ). Simulated results are reported as median values and interquartile ranges. No inferential statistical testing was performed, as this study represents a deterministic pharmacokinetic modeling analysis supplemented by stochastic simulation.

## Drug Selection and Pharmacologic Parameters

To capture a spectrum of molecular sizes, solubility profiles, and clearance behaviors encountered in intravitreal pharmacotherapy, two well-characterized agents were selected. These represent distinct pharmacologic classes and physicochemical properties: a lipophilic corticosteroid (Triamcinolone acetonide) and a hydrophilic glycopeptide antibiotic (Vancomycin).

## Pharmacokinetic Modeling

### Background and Standard Clinical Dosing

Intravitreal pharmacotherapy relies on small injection volumes (typically 0.05–0.1 mL) that deliver drugs directly into the vitreous cavity. In routine ophthalmic practice, dosing is highly standardized and currently not individualized for eye size. For both antibiotics and corticosteroids, the recommended intravitreal doses are derived from pivotal clinical studies rather than from pharmacokinetic scaling.

### Triamcinolone Acetonide

The standard human dose for posterior-segment diseases is 4 mg in 0.1 mL preservative-free suspension. This regimen has been consistently used in macular edema, diabetic retinopathy, and non-infectious posterior uveitis.<sup>29–31</sup> Studies confirmed a similar pharmacokinetic profile in vitrectomized eyes, establishing the 4 mg/0.1 mL bolus as the reference dose.<sup>32,33</sup> The formulation's high lipophilicity seems to result in depot behavior and prolonged retention within the vitreous and along retinal surfaces. However, 4 mg doses showed better clinical results in terms of anatomic outcomes, recurrence rates, and quality of life measures compared to 2 mg doses. It should be emphasized that none of these studies ever took vitreous volume into account or provided information on anatomical eyeball size.

### Vancomycin

For acute bacterial endophthalmitis, guidelines from the Endophthalmitis Vitrectomy Study (EVS) established the current empiric protocol of 1.0 mg in 0.1 mL for gram-positive coverage, usually combined with ceftazidime 2.25 mg/0.1 mL for gram-negative organisms.<sup>34,35</sup>

**Table 1** Initial Intravitreal Triamcinolone Acetonide Concentrations by Eye Size

Triamcinolone Acetonide (4 mg/0.1 mL)			
Eye size	Vitreous volume (mL)	Initial C <sub>0</sub> (mg/mL)	Relative to emmetropic (%)
Small (20 mm)	2.98	1.34	172%
Normal (23.5 mm)	5.12	0.78	100%
Large (30 mm)	11.76	0.34	44%

Subsequent pharmacokinetic analyses confirmed that this dose achieves therapeutic concentrations exceeding the minimum inhibitory concentration (MIC  $\approx$  0.005 mg/mL) for most gram-positive pathogens without retinal toxicity. Despite universal use of these fixed doses, the vitreous distribution volume differs more than fourfold among patients. It seems that past clinical studies regarding treatment intervals and dosage have not taken this into account.

## Results

### Size-Stratified Modeling for Triamcinolone Acetonide

For the reference 4 mg / 0.1 mL intravitreal dose, the calculated initial concentrations are 1.34 mg/mL in a small (20 mm) eye, 0.78 mg/mL in an emmetropic (23.5 mm) eye, and 0.34 mg/mL in a large (30 mm) eye (Table 1). With a vitreous half-life ( $t_{1/2}$ ) of  $\approx$  18 days, derived from human pharmacokinetic studies,<sup>29–31</sup> the first-order elimination model:  $C(t) = C_0 \cdot e^{(-0.0385 t)}$  predicts that the 0.1 mg/mL therapeutic threshold is crossed at approximately 67.4 days in small eyes, 53.4 days in normal eyes, and 31.8 days in large eyes. These values align with the established 6–8 week clinical duration of action for triamcinolone while demonstrating a substantial geometry-driven reduction in drug persistence (Figure 1).

Because  $C_0$  is inversely proportional to vitreous volume, larger eyes enter the exponential elimination phase from a lower starting point and therefore reach the therapeutic threshold markedly earlier despite identical half-life. In the present model, this corresponds to a  $\approx$ 40% shorter duration of action between normal and large eyes and a  $\approx$ 50% reduction between small and large eyes.

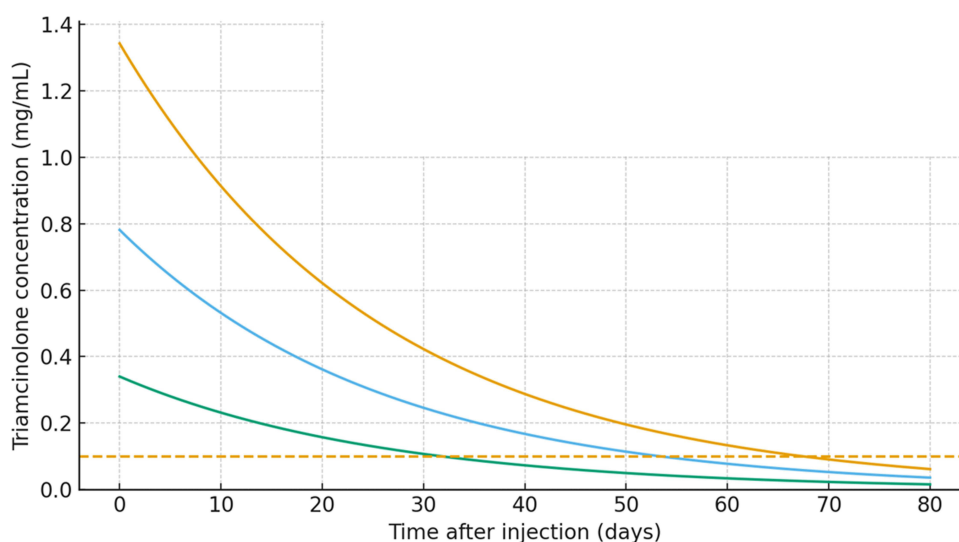


**Figure 1** Modeled intravitreal triamcinolone acetonide concentration–time profiles for three eye sizes based on VIVEX-derived vitreous volumes. A 4 mg/0.1 mL intravitreal bolus was simulated using a one-compartment first-order elimination model with a half-life of 18 days. Initial concentrations ( $C_0$ ) were 1.342 mg/mL in the small eye (AL 20 mm, VV 2.98 mL), 0.781 mg/mL in the normal eye (AL 23.5 mm, VV 5.12 mL), and 0.340 mg/mL in the large eye (AL 30 mm, VV 11.76 mL). The dashed horizontal line represents the therapeutic threshold of 0.1 mg/mL. The modeled duration above this threshold ( $\tau_{\text{eff}}$ ) was 67.4 days in small eyes, 53.4 days in normal eyes, and 31.8 days in large eyes, demonstrating a geometry-driven reduction of nearly 40% between hyperopic and highly myopic eyes despite identical dosing.

**Table 2** Initial Intravitreal Vancomycin Concentrations by Eye Size

Vancomycin (1 mg/0.1 mL)			
Eye size	Vitreous volume (mL)	Initial $C_0$ (mg/mL)	Relative to emmetropic (%)
Small (20 mm)	2.98	0.336	172%
Normal (23.5 mm)	5.12	0.195	100%
Large (30 mm)	11.76	0.085	44%

## Size-Stratified Modeling for Vancomycin

Using a clinically realistic minimum inhibitory concentration (MIC) of 0.005 mg/mL (5  $\mu$ g/mL), the modeled initial concentrations ( $C_0$ ) remained well above this threshold in all eye sizes, with 0.336 mg/mL in the small eye (VV 2.98 mL), 0.195 mg/mL in the normal eye (VV 5.12 mL), and 0.085 mg/mL in the large eye with VV 11.76 mL (Table 2). Despite this uniformly high starting level, the exponential decline caused by a short intravitreal half-life ( $t_{1/2} \approx 1.5$  days) resulted in markedly different durations of therapeutic exposure across geometries.

The effective duration of action above the MIC ( $t_{\text{eff}}$ ) was 9.1 days in small eyes, 7.9 days in normal eyes, and 6.1 days in large eyes, representing a geometry-driven reduction of approximately one third between hyperopic and highly myopic eyes. This contraction of the antibacterial exposure window arises solely from the dilutional effect of the enlarged vitreous cavity, as the elimination rate constant ( $k \approx 0.462 \text{ d}^{-1}$ ) remains identical across anatomies (Figure 2). Figure 2 illustrates the modeled concentration–time curves for the three VIVEX-derived vitreous volumes and highlights how the larger eye approaches the MIC earlier than the smaller eye despite identical dosing.

## Monte Carlo Simulation

In 10,000 simulated eyes ( $AL \sim N[23.5 \text{ mm}, 2.5 \text{ mm}]$ ), vitreous volumes showed a right-skewed distribution with a median of approximately 5.1 mL (IQR 3.9–6.7 mL). Across both modeled agents, anatomical variability resulted in an exposure (AUC) range of approximately  $0.68\times$  to  $1.32\times$  relative to the emmetropic reference, indicating that biometric variability accounts for roughly 30% of modeled pharmacokinetic variance.

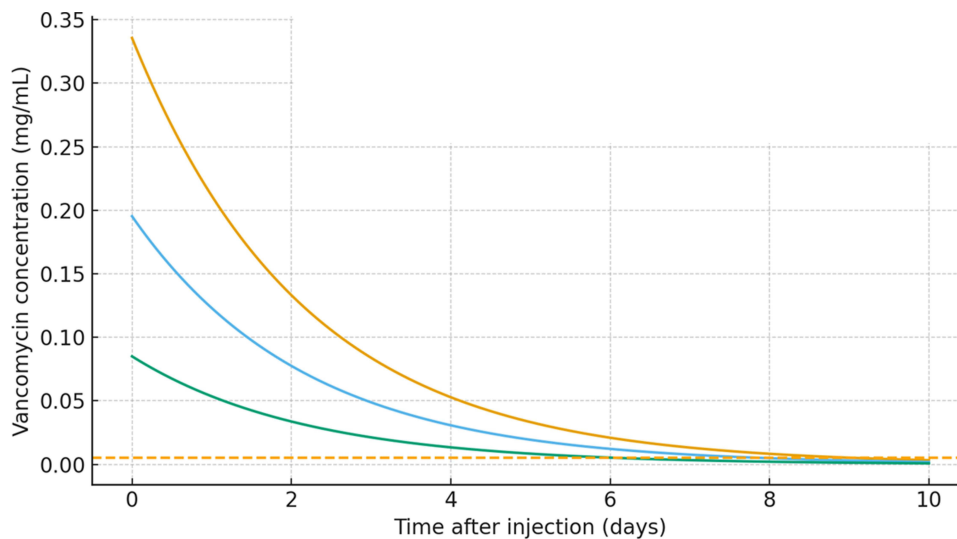


**Figure 2** Modeled intravitreal vancomycin concentration–time profiles for three eye sizes based on VIVEX-derived vitreous volumes. A 1 mg/0.1 mL intravitreal bolus was simulated using a one-compartment first-order elimination model with an intravitreal half-life of 1.5 days. Initial concentrations ( $C_0$ ) were 0.336 mg/mL (small eye, VV 2.98 mL), 0.195 mg/mL (normal eye, VV 5.12 mL), and 0.085 mg/mL (large eye, VV 11.76 mL). The dashed horizontal line represents the clinically realistic minimum inhibitory concentration (MIC) of 0.005 mg/mL (5  $\mu$ g/mL). While all eyes start far above the MIC, larger vitreous volumes lead to a faster decline toward this threshold, resulting in a shorter effective antibacterial exposure period in large myopic eyes.

## Discussion

In this work we try to make more clearly a point that is often overlooked in intravitreal therapy, namely how strongly the anatomy of the eye can influence the pharmacologic behavior of a drug. Anatomical variability in vitreous cavity volume is expected to influence the distribution, peak concentration, and elimination kinetics of intravitreally administered drugs. Under fixed dosing conditions, smaller eyes are predicted to experience higher initial concentrations and greater transient IOP elevations, whereas larger eyes exhibit increased dilution and earlier decline toward pharmacodynamic thresholds. The present modeling results quantify these geometry-driven effects. A 30-mm globe is not simply a “large eye”; it represents a fundamentally different pharmacokinetic environment, where any injected agent is diluted to one quarter of the concentration achieved in a 20-mm eye. This geometric disparity creates predictable differences in both efficacy and safety: small eyes are exposed to higher peaks and greater pressure load, whereas large eyes experience faster dilution, shorter therapeutic duration, and a narrower pharmacologic buffer. In this sense, anatomy does not merely influence pharmacology, it defines it.

### Vitreous Volume Scaling and Concentration Consequences

Using the VIVEX formula, vitreous cavity volume (VV) increases markedly with axial length (AL): approximately 2.98 mL at 20 mm, 5.12 mL at 23.5 mm, and 11.76 mL at 30 mm. These volumes correspond closely with MRI-derived normative data and with population studies of ocular geometry, confirming that the VIVEX-derived values realistically capture the anatomic variation between hyperopic and highly myopic eyes.<sup>12,13,36</sup> Because initial drug concentration follows  $C_0 = \text{Dose} / V$ , a fourfold range in VV inherently produces roughly fourfold variability in  $C_0$  across the modeled axial-length range. This anatomic scaling is directly propagated through the exponential elimination model  $C(t) = C_0 \cdot e^{-(kt)}$ , so that all subsequent pharmacokinetic metrics (AUC, time above a given threshold, and the effective safety margin) become functions of vitreous volume. In our simulations, this purely geometric effect translated into  $\approx 25\text{--}30\%$  differences in exposure between small and large eyes for identical doses and half-lives, even before considering any additional biological variability in clearance. To summarize the impact of geometry on the safety and efficacy margin, we defined a simple Vitreous Therapeutic Index ( $TI = C_0 / C_{\text{thresh}}$ ).

Beyond quantifying concentration differences, the introduction of the Vitreous Therapeutic Index (TI) and geometry-dependent duration provides a practical vocabulary for interpreting clinical variability. These metrics help explain why some patients exhibit early loss of effect or require unexpectedly frequent retreatment despite receiving standard doses: anatomical dilution shrinks both the pharmacologic buffer (TI) and the time above therapeutic thresholds ( $t_{\text{eff}}$ ). The ability to express these disparities numerically strengthens the framework for individualized dosing.

In the present model, TI for triamcinolone decreases from 13.4 to 3.4 when moving from small to large eyes, while TI for vancomycin decreases from 67.1 to 17.0 when using a MIC-based threshold of 0.005 mg/mL (Figures 3 and 4). TI represents a dimensionless concentration ratio ( $C_0 / C_{\text{thresh}}$ ) and is independent of exposure duration. This demonstrates that even though all eyes start far above the MIC, the pharmacologic buffer and duration of action shrink substantially with increasing vitreous volume, especially for short-acting hydrophilic antibiotics.

The modeled results demonstrate that fixed intravitreal dosing leads to substantial geometry-driven differences in drug exposure across eye sizes. Smaller eyes experience higher peak concentrations and longer duration above therapeutic thresholds, whereas larger eyes exhibit dilutional reduction in exposure and earlier decline toward pharmacodynamic targets. These effects are particularly pronounced for short-acting hydrophilic agents, where reduced initial concentration directly shortens effective exposure time.

For depot-forming corticosteroids, geometry predominantly influences peak concentration and retreatment interval, whereas for antibiotics with short intravitreal half-lives, vitreous volume directly determines the duration of effective antimicrobial coverage. In particular, the dilutional effect observed in larger eyes leads to a clinically relevant shortening of the effective antibacterial exposure window under fixed dosing conditions. These geometry-driven differences may help explain why highly myopic or vitrectomized eyes sometimes exhibit earlier microbiologic relapse and underscore the importance of close clinical reassessment when infection control appears suboptimal. The geometry-driven reduction in drug exposure and duration of action across different eye sizes is illustrated in Figures 5 and 6.

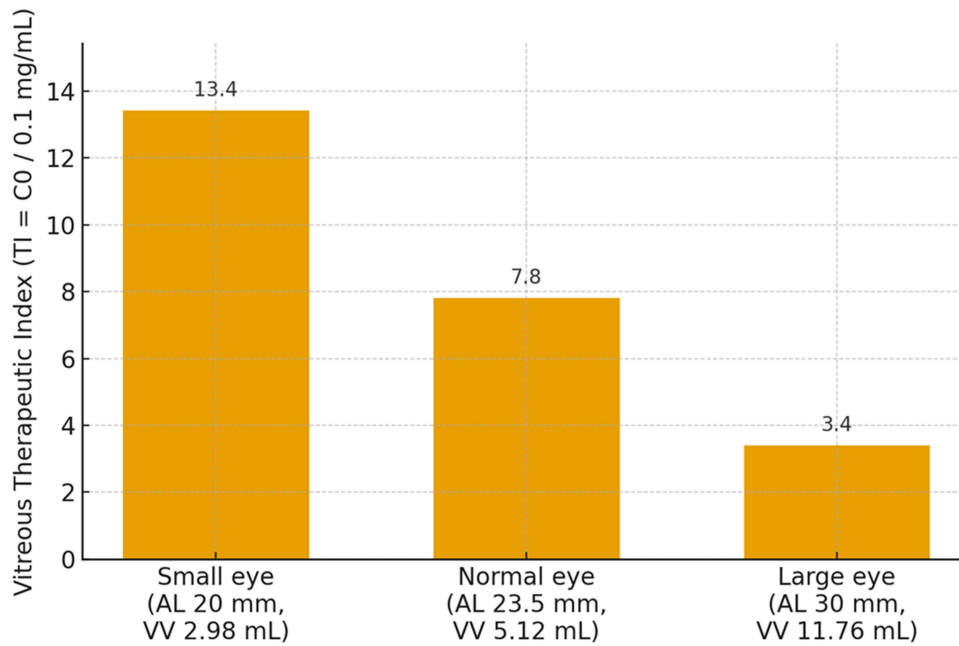


**Figure 3** Vitreous Therapeutic Index (TI) for triamcinolone acetate across three eye sizes based on VIVEX-derived vitreous volumes. TI was defined as the ratio between the initial intravitreal concentration  $C_0$  and a therapeutic threshold of 0.1 mg/mL ( $TI = C_0 / 0.1 \text{ mg/mL}$ ). A 4 mg/0.1 mL bolus injection was simulated for a small hyperopic eye (AL 20 mm, VV 2.98 mL,  $TI = 13.4$ ), a normal emmetropic eye (AL 23.5 mm, VV 5.12 mL,  $TI = 7.8$ ), and a large myopic eye (AL 30 mm, VV 11.76 mL,  $TI = 3.4$ ). The progressive reduction in TI with increasing vitreous volume illustrates the shrinking pharmacologic safety and efficacy margin in large eyes despite identical dosing.

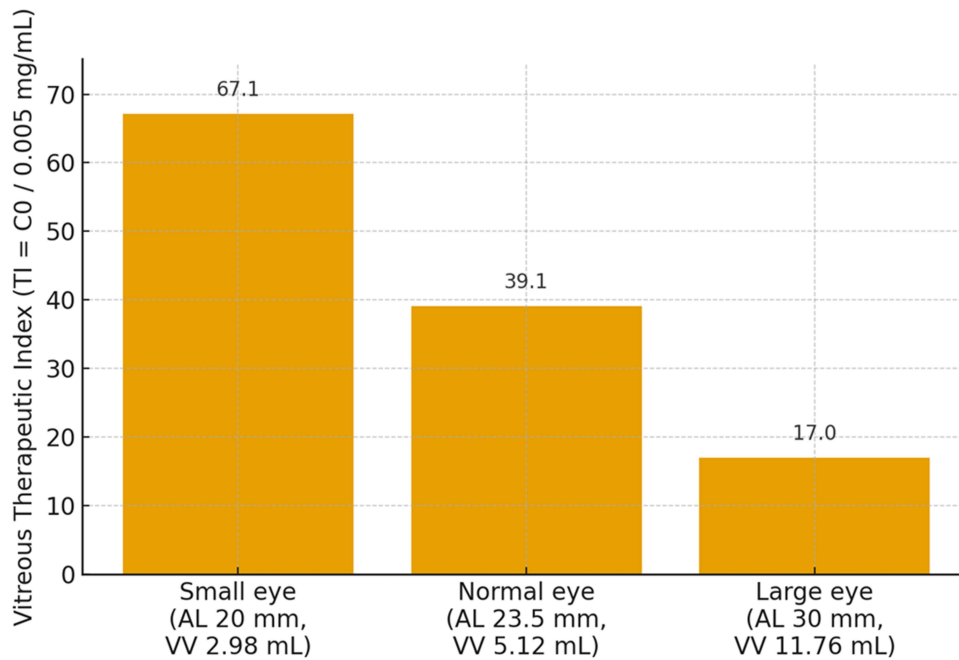


**Figure 4** Vitreous Therapeutic Index (TI) for vancomycin across three eye sizes based on VIVEX-derived vitreous volumes. TI was defined as the ratio between the initial intravitreal concentration  $C_0$  and a minimum inhibitory concentration (MIC) of 0.005 mg/mL (5  $\mu\text{g/mL}$ ). For a 1 mg/0.1 mL intravitreal bolus, TI values were 67.1, 39.1, and 17.0 in small (AL 20 mm, VV 2.98 mL), normal (AL 23.5 mm, VV 5.12 mL), and large (AL 30 mm, VV 11.76 mL) eyes, respectively. Although all eyes therefore start far above the MIC, the pharmacologic safety and efficacy margin shrinks markedly with increasing vitreous volume.

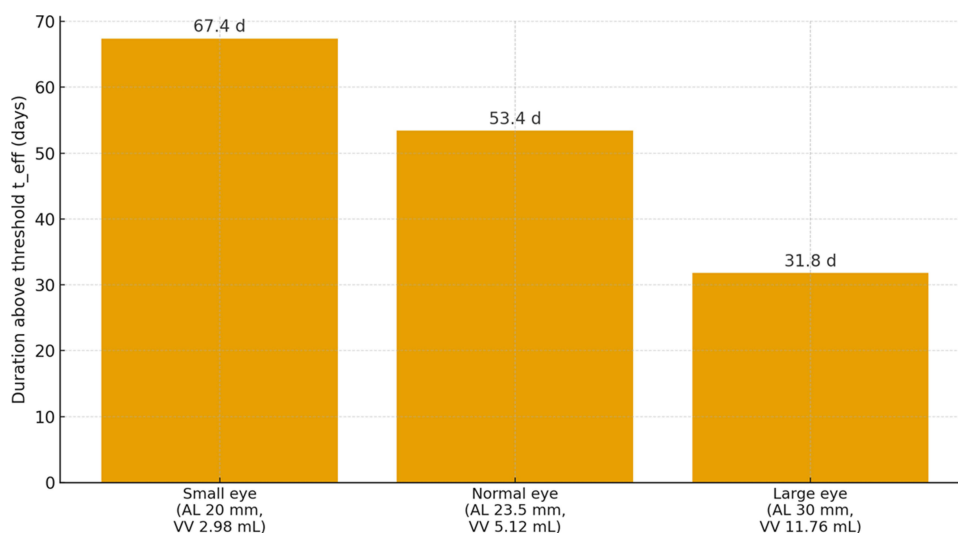


**Figure 5** Triamcinolone duration of action ( $t_{eff}$ ) across three eye sizes. The effective duration of action  $t_{eff}$  was defined as the time for which the modeled concentration remained above the therapeutic threshold of 0.1 mg/mL after a 4 mg/0.1 mL intravitreal bolus. Using VIVEX-derived vitreous volumes (2.98, 5.12, 11.76 mL),  $t_{eff}$  decreased from 67.4 days (small eye) to 53.4 days (normal eye) and 31.8 days (large eye), illustrating the geometric reduction in duration of action with increasing vitreous cavity volume.

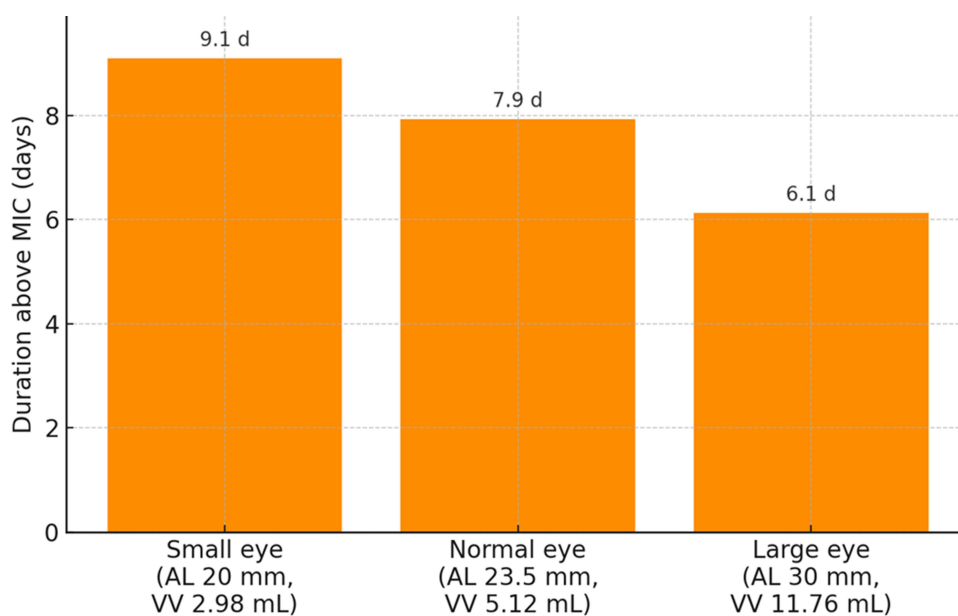


**Figure 6** Effective duration of action ( $t_{eff}$ ) for intravitreal vancomycin across three eye sizes.  $t_{eff}$  was defined as the time for which the modeled concentration remained above the MIC of 0.005 mg/mL (5  $\mu$ g/mL) after a 1 mg/0.1 mL bolus injection. Using VIVEX-derived vitreous volumes,  $t_{eff}$  was 9.1 days in the small eye (AL 20 mm, VV 2.98 mL), 7.9 days in the normal eye (AL 23.5 mm, VV 5.12 mL), and 6.1 days in the large eye (AL 30 mm, VV 11.76 mL). Thus, anatomical enlargement of the vitreous cavity shortens the effective antibacterial exposure window by roughly one third between small and large eyes, despite identical dosing and the same elimination half-life.

Because vancomycin is hydrophilic and eliminated via anterior aqueous outflow, its clearance depends almost entirely on cavity volume and outflow facility, not on tissue binding. Large eyes or those with liquefied vitreous therefore represent potential “underexposure” phenotypes, while smaller eyes receive higher effective concentrations with minimal additional toxicity risk.

### Transient Intraocular Pressure ( $\Delta$ IOP) Response

Modeled pressure increases using the ocular compliance relation ( $C \approx 0.02$  mL/mmHg) predict immediate  $\Delta$ IOP values of  $\approx 4.3$  mmHg in small eyes (VV = 2.98 mL),  $\approx 2.5$  mmHg in emmetropic eyes (VV = 5.12 mL), and  $\approx 1.1$ –1.5 mmHg

in large eyes ( $VV = 11.76$  mL). These values are consistent with clinical data for 0.05 mL injections and the observed correlation of post-injection IOP changes.<sup>37,38</sup>

In healthy, non-vitreotomized eyes, these transient elevations resolve within minutes as the injected volume redistributes and aqueous outflow compensates.<sup>39</sup> Nevertheless, in eyes with pre-existing glaucoma or compromised optic nerve head perfusion, small-volume anatomy can transiently elevate pressure to potentially risky levels.

## Monte Carlo Simulation

The Monte Carlo simulation supports vitreous volume as a clinically relevant contributor to inter-individual variability in intravitreal drug exposure. These findings suggest that a meaningful proportion of pharmacokinetic heterogeneity may arise from biometric differences rather than solely from molecular or disease-related factors. Incorporating ocular biometry into future pharmacokinetic and clinical trial models may therefore improve treatment consistency and reduce unexplained variability.

## Possible Clinical Interpretation

The theoretical model study demonstrates how axial length, an easily measurable biometric variable, translates into predictable differences in drug exposure and pressure dynamics. For triamcinolone, large eyes display a modest reduction in duration (~1–2 weeks), while small eyes show higher peaks and more pronounced transient IOP responses. For vancomycin, the geometry-driven dilution accelerates the decline toward the MIC, shortening the effective antimicrobial window by about one third between small and large eyes. These relationships illustrate that even under fixed dosing, anatomic variability can meaningfully alter both efficacy and safety outcomes. Conceptually, the duration of action for any intravitreal agent can be viewed as the time during which intraocular concentrations remain above a pharmacodynamically relevant threshold at the target site. In a simple first-order model,  $t_{\text{eff}}$  scales with both the elimination half-life and the logarithm of the ratio  $C_0/C_{\text{thresh}}$ ; because  $C_0$  is inversely proportional to vitreous volume, larger eyes will systematically exhibit shorter  $t_{\text{eff}}$  for a given dose and molecule. For long-acting depot steroids, this geometric effect modestly shortens the retreatment interval, whereas for short-acting antibiotics it can halve the effective antibacterial window between small and large eyes. This underscores that “one-volume-fits-all” dosing inevitably produces different functional durations of action across the anatomical spectrum.

## Implications for Study Design and Clinical Implementation

Most intravitreal drug trials and treatment protocols assume a constant vitreous volume of 4–5 mL for all eyes. Incorporating VV or AL as covariates could markedly improve the accuracy of pharmacokinetic and efficacy analyses. Prospective, biometry-stratified studies could test whether VV-adjusted dosing, for instance, 70–80% of the standard dose in small eyes and 130–140% in large eyes, reduces under- or overexposure. Embedding the VIVEX calculation directly into optical biometers or OCT platforms could provide instantaneous volumetric estimates and automated dosing suggestions. Real-time alerts such as “large eye > 10 mL → re-evaluate vancomycin at 24 h” or “small eye < 3.5 mL → monitor IOP” would operationalize individualized care without increasing procedural complexity. One of the major strengths of this approach is its practicality: axial length is already measured in nearly all ophthalmic clinics worldwide. Integrating this readily available biometric parameter into intravitreal dosing decisions represents a low-cost, high-impact modification that could substantially improve the safety, consistency, and durability of intravitreal therapy without altering established clinical workflows.

## Relation to Existing Intravitreal Anti-VEGF Pharmacokinetic Models

Recent pharmacokinetic and pharmacodynamic modeling studies of intravitreal anti-VEGF agents in neovascular age-related macular degeneration have used linear one-compartment models with first-order elimination and assumed a fixed vitreous volume of 4 mL for all eyes.<sup>40</sup> Our VIVEX-based framework is mathematically compatible with these approaches and can be viewed as an anatomical extension: by replacing the single fixed volume with VIVEX-derived vitreous volumes for small, normal and large eyes, the same equations would immediately yield eye-size-specific concentration–time profiles and times above VEGF-suppression thresholds. Although the present analysis focused on

triamcinolone acetonide and vancomycin, this illustrates how geometry-based scaling could be integrated into existing anti-VEGF PK/PD models to explore whether standard dosing intervals are truly pharmacokinetically equivalent across the full range of axial lengths.

## Independent Anatomical Validation

The geometric assumptions of the VIVEX formula are independently corroborated by both MRI-based human data and intraoperative measurements. De Silva et al reported mean MRI-derived VV of  $4.9 \pm 0.4$  mL for emmetropic eyes. Lira et al measured real-time infusion volumes during vitrectomy and derived a polynomial equation ( $R^2 \approx 0.95$ ) virtually identical in slope to the MRI-based VIVEX curve. Their volumes were only 5–10% lower, as expected because the post-vitrectomy cavity (VVS) excludes residual cortical vitreous.<sup>17</sup> This close agreement across different imaging and intraoperative methods provides strong validation for using axial length as a precise surrogate for vitreous volume in pharmacometric modeling.

There are recent studies addressing vitreous volume estimation and dosing considerations further highlight the clinical relevance of anatomical variability in intravitreal therapy. The importance of accurate intraocular volume assessment extends beyond routine anti-infective and corticosteroid therapy and may also be relevant in conditions requiring precise intravitreal drug exposure, such as intraocular lymphoma or other targeted treatments.<sup>41</sup> These emerging data support continued investigation into geometry-informed dosing strategies across different therapeutic indications. The citation of axial length–based vitreous volume estimation in recent literature like retinoblastoma chemotherapy research further illustrates the broader translational relevance of geometry-informed dosing approaches in intravitreal therapy.<sup>42</sup>

## Limitations

The present model assumes a homogeneous vitreous body, instantaneous mixing, and first-order elimination. Triamcinolone acetonide is administered as a crystalline suspension, and its elimination is primarily dissolution-limited rather than governed by a single monoexponential decay. The present model therefore reflects a “solution-equivalent” approximation of the steroid rather than the full multiphasic depot behavior. While this simplification may underestimate the absolute duration of steroid persistence, the relative geometric effect—shorter duration in larger vitreous volumes—remains valid because the dissolution volume itself scales with eye size.

Moreover, the model assumes a homogeneous gel-like vitreous with a constant elimination rate. However, high myopia is strongly associated with advanced vitreous liquefaction, which lowers viscosity and accelerates convective mixing and anterior clearance. In such eyes, the geometry-driven reduction in drug exposure predicted by this model likely represents a conservative estimate; real-world pharmacokinetic differences may be even greater.

Physiologic factors such as vitreous liquefaction, prior vitrectomy, tamponade, or silicone oil can modify clearance, particularly for hydrophilic agents. The assumed ocular compliance of  $\sim 0.02$  mL/mmHg introduces  $\pm 0.3$ – $0.5$  mmHg uncertainty in  $\Delta$ IOP predictions. Despite these simplifications, simulated concentrations and IOP changes remain within observed clinical ranges, supporting the model’s practical validity. However, the use of a linear ocular compliance factor ( $\approx 0.02$  mL/mmHg) likely underestimates acute post-injection pressure elevations in small, rigid eyes. According to Friedenwald’s nonlinear pressure–volume relationship, identical volume increments produce disproportionately higher IOP rises in short hyperopic globes. The safety implications reported in this study should therefore be interpreted as minimum-risk estimates rather than upper bounds. Although the present analysis is theoretical, its conclusions are biologically plausible and supported by convergent lines of evidence. The geometric predictions derived from the VIVEX formula closely align with MRI-based, CT-based, and intraoperative infusion-volume data, all of which demonstrate a near-identical cubic dependence between axial length and intraocular cavity volume. This agreement between theoretical modeling and empirical data underlines the robustness of the geometric assumptions and reinforces the relevance of anatomy-based pharmacokinetics.

## Conclusions

This theoretical pharmacokinetic modeling study demonstrates that anatomical variation in vitreous cavity volume substantially influences predicted intravitreal drug concentration, exposure duration, and transient intraocular pressure

response under fixed dosing conditions. Across the physiological range of axial length, identical injection volumes result in meaningful differences in peak concentration and time above pharmacodynamic thresholds.

These findings describe geometry-driven scaling effects derived from analytical modeling and should be interpreted as hypothesis-generating. The present study also shows that the VIVEX formula provides a practical and anatomically grounded method for estimating individual vitreous volume from routinely measured axial length, thereby offering a clinically accessible framework to account for inter-individual geometric variability.

While the present analysis does not constitute clinical validation, incorporating biometry-based volume estimation into pharmacokinetic considerations may represent a rational step toward more individualized intravitreal therapy. Prospective clinical studies are required to determine whether volume-adjusted dosing improves therapeutic consistency and safety in routine intravitreal antibiotic and corticosteroid treatment and to further explore integration of biometric parameters into pharmacokinetic, pharmacodynamic modeling frameworks. Incorporating VV-based scaling into clinical workflows could improve treatment consistency and safety and forms the logical next step toward personalized intravitreal therapy. Well-designed clinical studies with high number of cases should be performed. Future research should pursue prospective VV-stratified dosing studies for short-acting intravitreal antibiotics (eg., vancomycin, ceftazidime) to test efficacy and safety. Long-term follow-up of steroid implants or depot injections to quantify whether VV predicts retreatment intervals or the integration of formulas like the VIVEX-derived VV into PK/PD modeling and clinical trial covariate frameworks. Future research based on this concept could help to systematically evaluate how vitreous volume influences both therapeutic efficacy and potential adverse events, such as transient IOP spikes, localized toxicity from overexposure in small hyperopic eyes, or subtherapeutic dosing and shortened retreatment intervals in large myopic eyes. Establishing such evidence would not only validate the theoretical model but could also lead to dose-adjustment strategies tailored to ocular geometry, ultimately improving the safety, durability, and predictability of intravitreal pharmacotherapy.

## Data Sharing Statement

All data analyzed in this study are included in this article. Further inquiries can be directed to the corresponding author.

## Ethics Statement

This study involved no human participants, patient data, or identifiable specimens. As a purely theoretical modeling analysis based on published biometric and pharmacokinetic parameters, it did not require approval from an institutional review board or ethics committee.

## Author Contributions

All authors made a significant contribution to the work reported, whether that is in the conception, study design, execution, acquisition of data, analysis and interpretation, or in all these areas; took part in drafting, revising or critically reviewing the article; gave final approval of the version to be published; have agreed on the journal to which the article has been submitted; and agree to be accountable for all aspects of the work.

## Funding

No funding was received. All costs incurred for material, measurements and journal fees in the course of the project were covered privately by the author (AFB) without any external support.

## Disclosure

All authors report no conflicts of interest in this work.

---

## References

1. Grzybowski A, Told R, Sacu S, et al. Euretina board. 2018 update on intravitreal injections: euretina expert consensus recommendations. *Ophthalmologica*. 2018;239(4):181–193. doi:10.1159/000486145.

2. Martin DF. Evolution of intravitreal therapy for retinal diseases—From CMV to CNV: the LXXIV Edward Jackson memorial lecture. *Am J Ophthalmol.* 2018;191:xli–lviii. doi:10.1016/j.ajo.2017.12.019
3. Wong TY, Cheung CMG, Larsen M, Sharma S, Simó R. Diabetic retinopathy. *Nat Rev Dis Primers.* 2016;2(1):16012. doi:10.1038/nrdp.2016.12
4. Cai X, Wang J, Zhao J, Dang Y. Safety and efficacy of ranibizumab combined with dexamethasone intravitreal implant versus ranibizumab monotherapy for macular edema secondary to retinal vein occlusion: a 12-month prospective, randomized study. *Int Ophthalmol.* 2025;45(1):436. doi:10.1007/s10792-025-03794-x.
5. Zarranz-Ventura J, Garay-Aramburu G, Calvo P, et al. FRB Spain study group. Treatment intervals with first-generation anti-vascular endothelial growth factor drugs: evaluating the unmet need in a real-world neovascular age-related macular degeneration national database. *Eye.* 2025;39:3306–3313. doi:10.1038/s41433-025-03996-8
6. Daien V, Finger RP, Talks JS, et al. Evolution of treatment paradigms in neovascular age-related macular degeneration: a review of real-world evidence. *Br J Ophthalmol.* 2021;105(11):1475–1479. doi:10.1136/bjophthalmol-2020-317434.
7. Sunaga T, Maeda M, Saulle R, et al. Anti-vascular endothelial growth factor biosimilars for neovascular age-related macular degeneration. *Cochrane Database Syst Rev.* 2024;6(6):CD015804. doi:10.1002/14651858.CD015804.pub2.
8. Lam LA, Mehta S, Lad EM, Emerson GG, Jumper JM, Awh CC. task force on intravitreal injection supplemental services. Intravitreal injection therapy: current techniques and supplemental services. *J Vitreoretin Dis.* 2021;5(5):438–447. doi:10.1177/24741264211028441.
9. Borkenstein AF, Borkenstein E-M, Presser A. Calculated drug concentrations in currently available intravitreal therapies: determination of dilution factor and deviation from recommended doses. *Cureus.* 2024;16(7):e65888. doi:10.7759/cureus.65888.
10. Huang Y, Zhang Y, Chen W, et al. Estimation of vitreous chamber volume using axial length measurements. *J Craniofac Surg.* 2025;36(6):e631–e634. doi:10.1097/SCS.0000000000001109.
11. de Santana JM, Cordeiro GG, Soares DTC, Costa MR, Paasha da Costa Pinto A, Lira RPC. Use of axial length to estimate the vitreous chamber volume in pseudophakic. *Graefes Arch Clin Exp Ophthalmol.* 2021;259(6):1471–1475. doi:10.1007/s00417-020-04991-3.
12. Azhdam AM, Goldberg RA, Ugradar S. In vivo measurement of the human vitreous chamber volume using computed tomography imaging of 100 eyes. *Transl Vis Sci Technol.* 2020;9(1):2. doi:10.1167/tvst.9.1.2.
13. Borkenstein AF, Borkenstein E-M, Langenbucher A. VIVEX: a formula for calculating individual vitreous volume: a new approach towards tailored patient dosing regime in intravitreal therapy. *Ophthalmol Therapy.* 2024;13(1):205–219. doi:10.1007/s40123-023-00838-2.
14. Erduran B, Koçak N. Letter to the editor regarding “VIVEX: a formula for calculating individual vitreous volume: a new approach towards tailored patient dosing regime in intravitreal therapy”. *Ophthalmol Therapy.* 2024;13(8):2285–2286. doi:10.1007/s40123-024-00974-3.
15. Borkenstein AF, Borkenstein E-M, Langenbucher A. A response to: letter to the editor regarding “VIVEX—A formula for calculating individual vitreous volume: a new approach towards tailored patient dosing regime in intravitreal therapy”. *Ophthalmol Therapy.* 2024;13(8):2287–2292. doi:10.1007/s40123-024-00975-2.
16. Koçak N, Gürpınar A, Yeter Y. Effect of estimated individual vitreous volume on intraocular pressure spikes after intravitreal anti-vascular endothelial growth factors injection. *Ophthalmic Res.* 2025;68(1):108–116. doi:10.1159/000543071.
17. Lira RPC, Silveira APT, Lira GR, Gaete MIL. Dose adjustment of intravitreal medications and gases according to axial length and vitreous cavity volume. *Arq Bras Oftalmol.* 2025;88(6):e20250077. doi:10.5935/0004-2749.2025-0077.
18. Hu Q, Liu G, Deng Q, Wu Q, Tao Y, Jonas JB. Intravitreal vascular endothelial growth factor concentration and axial length. *Retina.* 2015;35(3):435–439. doi:10.1097/IAE.0000000000000329.
19. Sadeghi A, Subrizi A, Del Amo EM, Urtti A. Mathematical models of ocular drug delivery. *Invest Ophthalmol Vis Sci.* 2024;65(11):28. doi:10.1167/iops.65.11.28.
20. Maulvi FA, Shetty KH, Desai DT, Shah DO, Willcox MDP. Corrigendum to ‘Recent advances in ophthalmic preparations: ocular barriers, dosage forms and routes of administration’. *Int J Pharm.* 608 (2021) 121105. *Int J Pharm.* 2022;616:121583. doi:10.1016/j.ijpharm.2022.121583
21. Moisseiev E, Loewenstein A. Drug delivery to the posterior segment of the eye. *Dev Ophthalmol.* 2017;58:87–101. doi:10.1159/000455276
22. Jonas JB, Jonas RA, Panda-Jonas S. Clinical and histological aspects of the anatomy of myopia, myopic macular degeneration and myopia-associated optic neuropathy. *Prog Retin Eye Res.* 2025;109:101402. doi:10.1016/j.preteyeres.2025.101402
23. Tideman JWL, Polling JR, Vingerling JR, et al. Axial length growth and the risk of developing myopia in European children. *Acta Ophthalmol.* 2018;96(3):301–309. doi:10.1111/aos.13603.
24. Tojo KJ, Ohtori A. Pharmacokinetic model of intravitreal drug injection. *Math Biosci.* 1994;123(1):59–75. doi:10.1016/0025-5564(94)90018-3.
25. Tojo K, Isowaki A. Pharmacokinetic model for in vivo/in vitro correlation of intravitreal drug delivery. *Adv Drug Deliv Rev.* 2001;52(1):17–24. doi:10.1016/s0169-409x(01)00187-9.
26. Zhang Y, Bazzazi H, e Silva RL, et al. Three-dimensional transport model for intravitreal and suprachoroidal drug injection. *Invest Ophthalmol Vis Sci.* 2018;59(12):5266–5276. doi:10.1167/iops.17-23632.
27. Meyer CH, Krohne TU, Charbel Issa P, Liu Z, Holz FG. Routes for drug delivery to the eye and retina: intravitreal injections. *Dev Ophthalmol.* 2016;55:63–70. doi:10.1159/000431143
28. Barza M. Pharmacokinetics of newer cephalosporins after subconjunctival and intravitreal injection in rabbits. *Arch Ophthalmol.* 1993;111(1):121–125. doi:10.1001/archophth.1993.01090010125038.
29. Beer PM, Bakri SJ, Singh RJ, Liu W, Peters GB 3rd, Miller M. Intraocular concentration and pharmacokinetics of triamcinolone acetonide after a single intravitreal injection. *Ophthalmology.* 2003;110(4):681–686. doi:10.1016/S0161-6420(02)01969-3.
30. Jonas JB. Intravitreal triamcinolone acetonide for treatment of intraocular oedematous and neovascular diseases. *Acta Ophthalmol Scand.* 2005;83(6):645–663. doi:10.1111/j.1600-0420.2005.00592.x.
31. Jonas JB. Intraocular availability of triamcinolone acetonide after intravitreal injection. *Am J Ophthalmol.* 2004;137(3):560–562. doi:10.1016/j.ajo.2003.08.012.
32. Rittiphairoj T, Mir TA, Li T, Virgili G. Intravitreal steroids for macular edema in diabetes. *Cochrane Database Syst Rev.* 2020;11(11):CD005656. doi:10.1002/14651858.CD005656.pub3.
33. Eduardo de Souza C, Zanetti Patricio de Macedo B, Viana de Sousa M, Naomi Morimoto L, Lima LH, Muccioli C. Treatment of non-infectious uveitis macular edema using two doses of triamcinolone acetonide: comparative study. *Ocul Immunol Inflamm.* 2025;33(7):1340–1348. doi:10.1080/09273948.2025.2504580.
34. Vaziri K, Schwartz SG, Kishor K, Flynn HW Jr. Endophthalmitis: state of the art. *Clin Ophthalmol.* 2015;9:95–108. doi:10.2147/OPHT.S76406

35. Tranos P, Dervenis N, Vakalis AN, Asteriadis S, Stavrakas P, Konstas AGP. Current perspectives of prophylaxis and management of acute infective endophthalmitis. *Adv Ther.* 2016;33(5):727–746. doi:10.1007/s12325-016-0307-8.
36. Jonas JB, Bikbov MM, Wang Y-X, Jonas RA, Panda-Jonas S. Anatomic peculiarities associated with axial elongation of the myopic eye. *J Clin Med.* 2023;12(4):1317. doi:10.3390/jcm12041317.
37. Gumus G, Berhuni M, Ozturkmen C. The short-term effects of intravitreal bevacizumab injection on intraocular pressure, cornea, iridocorneal angle, and anterior chamber. *Therapeutic Adv ophthalmol.* 2022;14:25158414221133772. doi:10.1177/25158414221133772
38. Özer Özcan Z, Gürbostan Soysal G, Tiskaoğlu NS, Berhuni M. The effect of baseline intraocular pressure and anterior segment parameters on intraocular pressure after intravitreal bevacizumab injection. *Cutan Ocul Toxicol.* 2023;42(4):248–252. doi:10.1080/15569527.2023.2243505.
39. Falkenstein IA, Cheng L, Freeman WR. Changes of intraocular pressure after intravitreal injection of bevacizumab (avastin). *Retina.* 2007;27(8):1044–1047. doi:10.1097/IAE.0b013e3180592ba6.
40. García-Quintanilla L, Luaces-Rodríguez A, Gil-Martínez M, et al. Pharmacokinetics of intravitreal anti-VEGF drugs in age-related macular degeneration. *Pharmaceutics.* 2019;11(8):365. doi:10.3390/pharmaceutics11080365.
41. de Smet MD. Die intravitreale Behandlung des okulären Lymphoms sollte angepasste Wirkstoffkonzentrationen und keine festen Dosierungen verwenden. *Klin Monbl Augenheilkd.* 2026. German. doi:10.1055/a-2788-0429
42. Tseng P-J, Sinenko IL, Chambon M, et al. High-throughput screening of drug libraries identifies a new synergistic drug combination for the treatment of retinoblastoma. *PLoS One.* 2026;21(2):e0339334. doi:10.1371/journal.pone.0339334

## Clinical Ophthalmology

### Publish your work in this journal

Clinical Ophthalmology is an international, peer-reviewed journal covering all subspecialties within ophthalmology. Key topics include: Optometry; Visual science; Pharmacology and drug therapy in eye diseases; Basic Sciences; Primary and Secondary eye care; Patient Safety and Quality of Care Improvements. This journal is indexed on PubMed Central and CAS, and is the official journal of The Society of Clinical Ophthalmology (SCO). The manuscript management system is completely online and includes a very quick and fair peer-review system, which is all easy to use. Visit <http://www.dovepress.com/testimonials.php> to read real quotes from published authors.

Submit your manuscript here: <https://www.dovepress.com/clinical-ophthalmology-journal>

**Dovepress**

Taylor & Francis Group